

Vehicle Tracking using Ultrasonic Sensors & Joined Particle Weighting

Philipp Köhler, Christian Connette, Alexander Verl

Abstract—In recent years, driver-assistance systems have emerged as one major possibility to increase comfort and safety in road traffic. Still, cost is one major hindrance to the widespread use of safety systems such as lane-change or blind spot warning. To facilitate the widespread adoption of such safety systems, thus increasing safety for all traffic participants, the use of cost-efficient components is of crucial importance.

Within this work we investigate the use of cost-efficient, widely used ultrasonic sensors for the tracking of passing-by vehicles at high velocities. Therefore, a particle filter with some mixture tracking capabilities is implemented to fuse the signals from 6 us-sensors. The main focus of this work lies on the development of a more detailed sensor model that is used in this particle filter. Additionally, a strategy to take into account object-visibility w.r.t. the different sensors is outlined. The derived concept is evaluated experimentally in real road traffic. The applicability of the tracking result in context of lane-change-decision-aid and blind-spot-surveillance systems is analyzed.

I. INTRODUCTION

During the last decade, autonomous driving has seen significant progress from the first DARPA Grand Challenges in 2004 and 2005 [1], [2], [3] over the DARPA Urban Challenge [4], [5] up to Google’s driverless car [6] which did hit the road about two years ago. Still it seems that legal considerations and costs might be an insurmountable obstacle to the commercialization of autonomous driving for quite some time. Yet, by now the developed concepts are hitting the road in form of driver-assistance systems and they emerge as one major possibility to increase both comfort and safety in road traffic [7]. The most repressing factor to the spread of driver-assistance systems in general, is their high costs. For instance, lane-change-decision-aid systems are usually based on camera [8], [9], lidar and radar systems [10] or some combination of those.

To foster the widespread use of driver-assistance systems it is important to reduce hardware cost by employing cost-efficient sensors or if possible sensors that are already ubiquitous in modern cars. Ultrasonic sensors do for instance already meet these requirements. They are comparably cost-efficient and already used in context of parking-aid systems [11]. However, the performance of us-sensors varies greatly depending on weather conditions [12]. They are sensitive to rain, spray or gusts of wind. Moreover, the amount of information that can be acquired is quite sparse. Us-sensors often have a wide aperture and a restricted range which makes it difficult to locate and track the source of an echo accurately.

This work was conducted in the department of Robot and Assistance Systems at the Fraunhofer Institute for Manufacturing Engineering and Automation (IPA), 70569 Stuttgart, Germany; Contact: phone: +49 711 970 1325; e-mail: christian.connette@ipa.fraunhofer.de

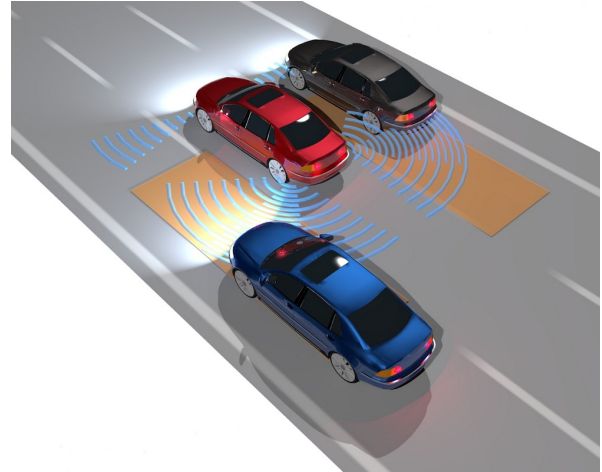


Fig. 1. The lower car (blue) is in the blind spot of the host-car’s (red) driver. The blue arcs depict the sensor range of the host-car’s us-sensors. The orange rectangles depict the critical zone which should be supervised.

Accordingly, the usage of ultrasonic sensors in context of novel driver-assistance systems was mainly focused on the detection of fast vehicles but rather not on their tracking. For instance, a fuzzy-markov based approach using an inverse-geometric model that reached notably detection rates was presented in [13]. Mirus et al. proposed a detector that uses artificial neural network to perform curve fitting of us-sensor data to different premodeled cases of different objects in the blind spot zone [14].

The work at hand investigates the tracking problem for fast vehicles in the vicinity of the host car up to absolute velocities of 160 km/h when using ultrasonic sensors. It applies a particle filter algorithm [15] with some mixture tracking capabilities [16] to perform Bayesian filtering in terms of monte carlo sampling. The primary contribution of this work is the development of an adapted us-sensor measurement model based on the model proposed by Thrun et al. in [17]. Additionally, a weighting strategy for the measurement step is proposed that implicitly leads to a tighter coupling of the separate ultrasonic sensors. This improves direction and velocity estimation in a fashion similar to sensor-arrays.

The remainder of the paper is organized as follows: In Sect. II the tracking problem is discussed w.r.t. particle filtering and mixture tracking. Sect. III describes the developed measurement and sensor models. In Sect. IV the tracking capabilities of the filter are analyzed and statistical detection results are shown. Sect. V concludes the work and gives possible further improvements and a prospect.

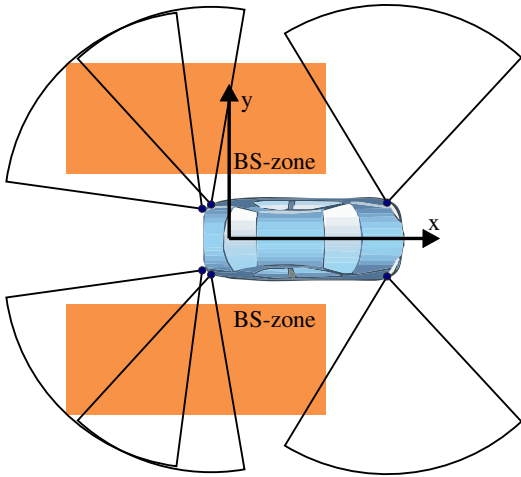


Fig. 2. Coverage of the used ultrasonic sensors (black arcs) and the blind spot zone. The coordinate-system is fixed to the host car as shown and is the base system for the particle filter.

II. PROBLEM STATEMENT

A. System Setup

The host car is equipped with an array of 12 ultrasonic sensors. The single sensors are placed equally on its front and rear. Within this work only six of them are used, three on each side of the car: the front-side and the rear sensor (aperture 75°) and additionally the passive rear-side sensor (aperture 50°), which only receives ultrasonic echoes emitted by the rear sensor (Fig. 2). All sensors are operating at a rate of 30 ms.

The region of special interest for lane-change maneuvers and in which objects shall be tracked is depicted in figure 1. It reaches (back to front) from 3 m behind the car up to the side mirrors and covers roughly three to four meters to the side. Ideally, a possible track should converge within 0.3 s after a car has entered this region. The system should operate under different weather conditions and in diverse environments (city, rural roads, autobahn). However, in the following we will focus on high-speed scenarios on the autobahn under mild weather conditions. This means heavy rain or snow will not be taken into account.

B. Vehicle Tracking with Ultrasonic Sensors

Typically, vehicle detection and tracking is separated in two individual steps using high-resolution sensor data like laser-range-scans [18], [19] to first detect an object and then feed this estimate to a tracking filter. Due to the very limited information that can be gathered from us-sensors, our approach dispenses with data segmentation, data association or separated detection. In contrast, the data from all sensors is merged immediately into one common state-space. As there might be more than one object – it is usually one or two – in the region of interest the resulting probability density function to represent the track might take the form of a multimodal distribution. Therefore, a particle filter with some mixture tracking capabilities was chosen to implement the tracking algorithm.

C. Particle Filter Setup & Model Assumptions

Our experiments and simulations have shown that it is usually sufficient to model a passing vehicle as an object that is moving parallel to the host car. To allow the representation of the approach-process which occurs during lane-change maneuvers of host or target car, a slight motion of the object in y -direction is accepted. Thus, a single particle is at time t represented via the four-dimensional vector

$$X_t = (x_t, y_t, v_{x,t}, v_{y,t})^T.$$

As detailed motion of the object is unknown the motion model is assumed to be linear and is perturbed by additional noise

$$X_{t,i} = AX_{t-1,i} + \Delta_{t,i} \quad (1)$$

to take into account the model uncertainties [18]. The perturbing value $\Delta_{t,i}$ is generated by drawing from a random variable with Gaussian distribution for the position variables. For the velocity variables a uniform distribution is taken as a basis to account for expected bounded target acceleration. Applying this motion model to every particle leads to an approximation of the probability density function $p(X_t | X_{t-1})$ representing the a priori estimate of moving objects in the vicinity of the host car.

One known issue of using particle filters for multi-target-tracking – especially in context with noisy sensors – is that one mode or particle cluster might cannibalize other clusters. Thus, the actual filter was implemented as a mixture model particle filter according to Vermaak et al. [16]. Therefore, the observation space was split into two areas separating the particles to a front and a rear cluster. For each of this clusters c_m an individual a posteriori probability distribution $p_m(X_t | Z_t)$ is approximated via its own normalized particle distribution

$$p_m(X_t | Z_t) = \sum_{i \in I_m} w_t^{(i)} \delta_{x_t^{(i)}}(X_t), \quad (2)$$

where $\delta_a(\cdot)$ is the Dirac delta measure with mass at a and I_m is the set of indices of the particles belonging to the m -th mixture component. The individual particle weight is a function of the inverted sensor model

$$w_t^{(i)} = p(Z_t | x_t^{(i)}). \quad (3)$$

The combined probability density may then be formed by calculating a weighted sum of both particle distributions following [16] to maintain a correctly normalized particle distribution at any time.

The implementation of the mixture model particle filter also simplifies adaptation of the birth process. New particles are spread within both of the two clusters taking into account the current sensor measurements via the inverted measurement model given in Sect. III-A. Thus, it is more straight forward to take into account that cars might approach the host car either from the front or from the back.

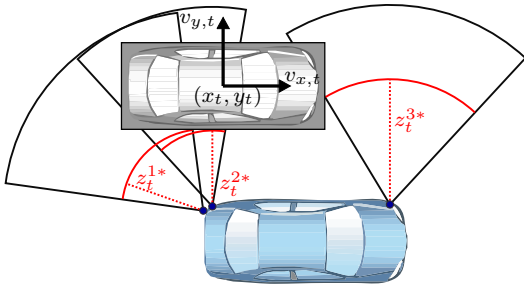


Fig. 3. Distances z_t^{k*} are the expected range scans for a sample vehicle. For a given (x_t, y_t) these expected distances arise from the intersection between the rectangle and the sensor cones.

III. JOINED PARTICLE WEIGHTING

A. Sensor Measurement Model

The basis of the particle filter estimation or weighting process is the calculation of the probability density $p(Z_t | X_t)$ of the obtained set of measurements Z_t for the current set of particles X_t . Assuming independence of the sensor readings this boils down to the calculation of the probability densities $p(z_t^k | X_t)$ for the separate measurements z_t^k originating from the K independent sensors for the given set of particles X_t . This calculation requires a model of the measurement process as well as the sensor characteristics.

To model the measurement process it is assumed that an ultrasonic range sensor will always return the distance to the closest surface of the objects in its coverage area. Within the work at hand the target vehicles geometry is simply modeled rectangular with fixed size. Thus, for a given X_t the expected measurement z_t^{k*} will be calculated as the shortest distance between the sensor and the intersection of the vehicles rectangle with the sensor cone (see Fig. 3).

The sensor characteristics are represented according to the classical model proposed by Thrun et al. in [17]. This model takes into account four different types of measurement errors: measurement noise, errors due to short readings, errors due to measurement failures, and tiny random unexplained noise. In the presented setup short reading errors and measurement failures resulting in max-range-readings are of particular interest. The resulting density $p(z_t^k | X_t)$ is then a mixture of this four densities, namely

- p_{hit} (narrow Gaussian around z_t^{k*} with standard deviation σ_{hit})
- p_{short} (exponential distribution for $z_t^k < z_t^{k*}$)
- p_{max} (1 if $z_t^k = z_{\text{max}}$)
- p_{rand} (uniform distribution).

To form the actual sensor model these densities are weighted via the tuning variables z_{hit} , z_{short} , z_{max} and z_{rand} for which holds

$$z_{\text{hit}} + z_{\text{short}} + z_{\text{max}} + z_{\text{rand}} = 1 \quad (4)$$

and summed up to the resulting measurement probability density function (Fig. 4).

B. Particle Weighting via Joined Inverse Sensor Models

Incorporating measurements to the particle filter is done by weighting each particle according to the measurement

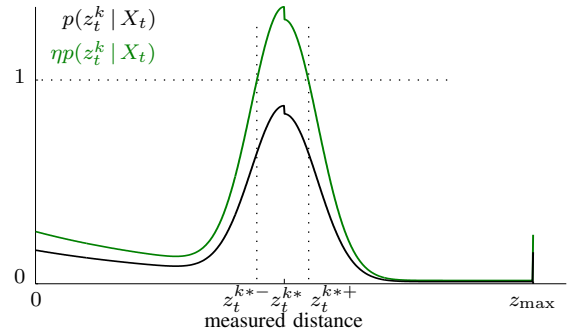


Fig. 4. Mixture probability density function that models four different types of measurement errors (namely measurement noise, short readings, measurement failures and random noise). The η -scaled density possesses an equilibrium – measurements between $z_t^{k*-/+}$ result in supporting weights.

probability. Therefore, the weight resulting from each single sensor will be calculated by evaluating the probability density for the actual obtained measurement

$$\tilde{w}_k^{(i)} = P(z_t^k | x_t^{(i)}) . \quad (5)$$

Fusion of the different sensor readings will usually be performed by multiplying the weights obtained for a single particle

$$\tilde{w}^{(i)} = \prod_{k=1}^3 \tilde{w}_k^{(i)} . \quad (6)$$

However, this implicitly assumes mutual independence of the incorporated sensors. In general, this will not be the case for measurements originating from one single object. Practically speaking: Usually, a specific particle will not be in the field of view of all sensors, but of some.

Naturally, a particle being supported by more sensors should earn a greater weight value than a particle only supported by one. But depending on the measurement function this desirable manner is harmed by simply multiplying the weights. If the peak value of the associated density is below 1 ($\max\{p(z_t^k | X_t)\} < 1$) this is even the case for measurements perfectly fitting the expected ones. This characteristics can be set aright by introducing an additional tuning parameter η . Each weight is now multiplied with this factor η – from another perspective this is scaling the measurement density function. The range of weights now contains 1.0 as neutral element for multiplication; measurements between z_t^{k*-} and z_t^{k*+} now explicitly result in supporting weights (Fig. 4). Adjusting the range of weights using the scaling factor η allows to tune this behavior by defining an equilibrium or "neutral" weight.

The desired manner for combining multiple sensor measurements on a single particle is then achieved by calculating a joined particle weight $w^{(i)}$

$$\hat{w}_k^{(i)} = (\eta \tilde{w}_k^{(i)})^{q_k} \quad (7)$$

$$\hat{w}^{(i)} = \prod_{k=1}^3 \hat{w}_k^{(i)} \quad (8)$$

$$w^{(i)} = \frac{\hat{w}^{(i)}}{\sum_{j=1}^N \hat{w}^{(j)}} , \quad (9)$$

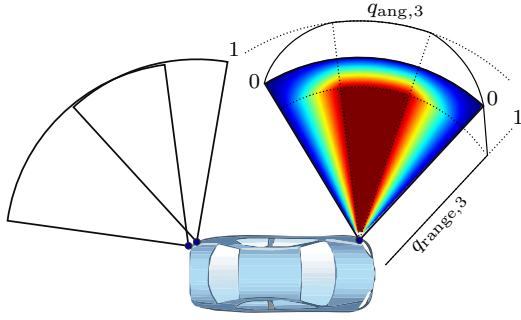


Fig. 5. Gradient of the reliability value depending on the expected origin of the sensor measurement. Angular and radial reliability values are determined separately and then joined multiplicatively to the resulting reliability value shown in color.

where (9) normalizes the weighted particle distribution.

The proposed classical measurement model in Sect. III-A penalizes only measurement derivations but takes not into account sensor reliability. Therefore $q_k^{(i)} \in [0, 1]$ was appended to the particle weighting procedure (7). Therein $q_k^{(i)}$ represents a sensor reliability value that indicates whether the vehicle which is represented by particle i is expected to be observed by sensor k . If the reliability to observe this particle is high, $q_k^{(i)}$ will become 1. If the reliability is very low, $q_k^{(i)}$ will become 0. By raising each measurements weight $\hat{w}_k^{(i)}$ to the power of the sensors reliability value, a sensor with a very low reliability will shift the outcome towards the equilibrium weight – and so influences the result of the joined weight for that particle only slightly. One possibility to calculate $q_k^{(i)}$ will be outlined in the next section.

Having created an equilibrium element for joined particle weighting makes it possible to incorporate this aspect directly into the particle filter framework.

C. Sensor Reliability Model

Our experiments have shown that objects close to the sensor cone border or close to the maximum range of the sensor produce only very unstable echoes. This is obvious as one must not forget that the cone model is only a rough representation of the propagation of ultrasonic waves which actually form lobes emanating from the sensor. To calculate the sensor reliability a characteristic angular coordinate

$$\hat{z}_t^{k*} = (\alpha_t^{k*}, z_t^{k*})^T \quad (10)$$

representing the reflecting surface within the sensor cone is calculated. Herein α_t^{k*} denotes the maximum angular distance to the sensor cone borders. It is calculated using the rectangular vehicle model, thus investigating that point of the rectangle that is closest to the sensor's direction. Analogously the expected minimal radial distance z_t^{k*} is calculated. Based on these values an angular reliability factor $q_{ang,k} \in [0, 1]$ and a radial reliability factor $q_{range,k} \in [0, 1]$ is determined. These may now be used to calculate the final combined reliability factor.

Within the work at hand the reliability factors were determined by applying a trapezoidal function over the sensor coverage area (see $q_{ang,3}$ and $q_{range,3}$ in Fig. 5). The

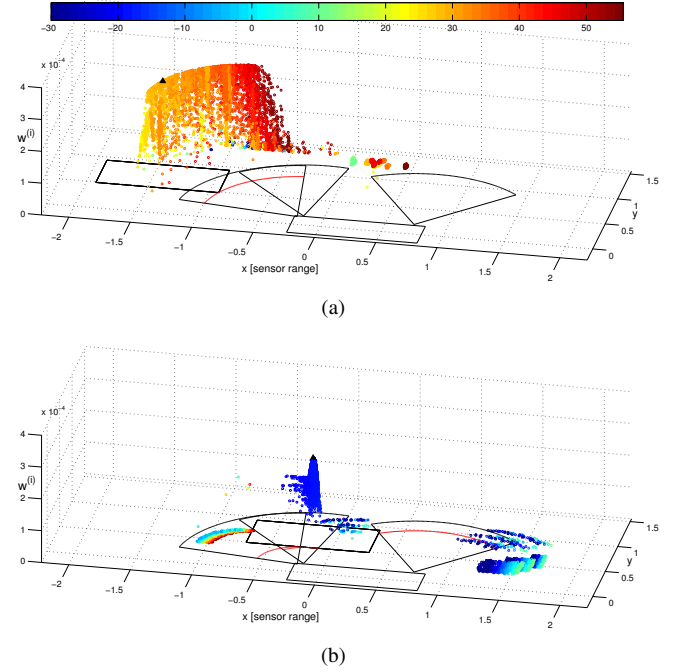


Fig. 6. Particle distribution of simulated measurement data ($v_{x,host} = 17$ m/s) with the simulated target marked. Z-coordinate of each particle shows its weight, color is representing velocity in [m/s]. In (a) a target vehicle is entering the FOV from behind ($v_x = 30$ m/s), in (b) a target vehicle is passing in the opposite direction ($v_x = -10$ m/s) (as correctly shown by the particles negative velocities).

calculation of the combined reliability factor is performed by simply multiplying angular and radial reliability factor

$$q_k = q_{ang,k}(\alpha_t^{k*}) \cdot q_{range,k}(z_t^{k*}) \quad (11)$$

IV. EXPERIMENTAL RESULTS

To quantify tracking and detection performance the host car was equipped with two laserscanners. The obtained data was annotated manually. In total more than 500 use cases were annotated to check detection performance. About 40 use cases were additionally annotated in detail at intervals of 1 m to allow assessment of the tracking performance. While tracking performance is of specific interest for the work at hand the evaluation of the detection performance gives a good hint in how far the proposed algorithm may be applied in context of driver-assistance systems such as lane-change-decision-aid systems or blind-spot-surveillance systems.

A. Tracking Results

Fig. 7 shows a sample scene of an overtaking car on a motorway. The resulting particle densities demonstrate that our filter is able to propagate a dense particle cluster representing the target vehicle through the observation space. The densities display some limitations mainly resulting from the sparse sensor information: In Fig. 7(a) the track initially forms as an arc since there is no additional sensor information available to limit the degree of freedom of the particles. The velocity of the particles is being fixed in this phase depending on their position on the arc (see also Fig. 6(a)). The best estimate of a vehicle's position can be obtained

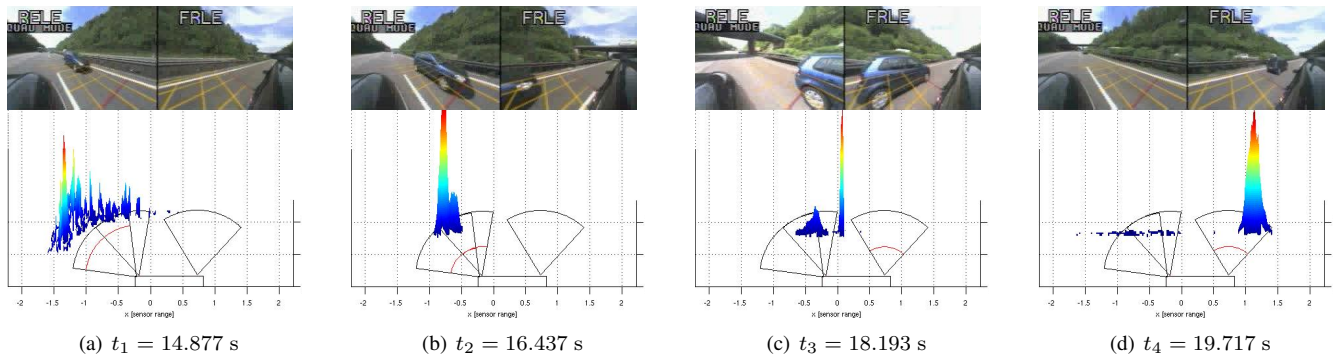


Fig. 7. A target vehicle passing the host car on the left. The video frames originate from the roof-mounted color camera and show view to the front (FRLE) and rear (RELE). Below the correspondent grid-based particle densities are shown. The density per grid cell is color encoded where dark-blue means lowest density. Red arcs symbolize actual sensor measurements.

while it is passing the side of the host car (Fig. 7(c)). Finally, when the target is only in the front sensors FOV, the track again becomes more uncertain (now in x -direction due to lateral acceleration and deceleration according to the vehicle dynamics model, Fig. 7(d)).

Figure 8 depicts mean and standard-deviation of the tracking error obtained for 41 tracking-cases with and without the joined particle weighting proposed in section III-C. It becomes apparent that the introduction of the sensor reliability model and the joined particle weighting enhances tracking of a vehicle significantly. Especially a "soft" angular reliability-border of the front sensor favors a smooth propagation of particles throughout the observation space. The eminent effect of the sensors "soft" borders has its seeds not only in the presence of measurement errors but results also from cushioning modelling errors rising from different real-vehicle lengths.

B. Vehicle Detection in Application Context

To evaluate the tracking result w.r.t. its applicability to vehicle detection a simple detector-module that overlays the particle filter was implemented. Several properties of the particle distribution are used for determining whether a target vehicle is present in the blind spot area or not. A necessary condition for this is certainly the presence of any vehicle in the field of view that is reflected by any spatial convergence of the particle distribution in combination with persistent high unnormalized weights $\hat{w}^{(i)}$. This criteria makes it also possible to distinguish between a vehicle and any spuriously tracked infrastructure that does not match the geometry assumed for a vehicle. For each vehicle hypothesis the velocity estimate is evaluated to discriminate between a parking vehicle, one passing in the opposite direction or again just tracked infrastructure (Fig. 6(b)).

To assess capability and performance of the proposed procedure in the BSD-scenario extensive testing has been conducted. The test set presented in figure 9 contains about 221 km of motorway data including 535 use cases. On the whole test set, a total detection rate of 97.38 % and a false alarm rate of 6.96 % was reached.

In table I the detection rate for some motorbike testcases (40 cases in total) are given. This is a stresstest to the

proposed approach as motorbikes offer a very bad reflection face to ultrasonic waves and thus lead to instable and noisy echoes. Yet, the proposed model-based detection approach shows quite good results with an overall detection rate of 97.5 % and a false-alarm rate of 5 % (two false alarms).

TABLE I
DETECTION RATES AND TIMES ON A MOTORBIKE TEST SET

| Reaction time | $t < 0.3$ s | $t < 0.6$ s | $t < 1.5$ s | no limit |
|----------------|-------------|-------------|-------------|----------|
| Detection rate | 90.0% | 90.0% | 95.0% | 97.5% |

V. CONCLUSION & OUTLOOK

The evaluation of the tracking performance as well as the detection rate of the presented particle filter approach delivered promising results. Especially in motorway conditions our algorithm performs solid tracking and returns fast blind spot warnings. Inner city and heavy rain conditions still pose a challenge mainly to false detections. One idea to tackle these difficulties could be to have multiple parameter sets for the particle filter and the detection module adjusted to the different conditions.

Another topic that seems to be worth further investigation is the enhanced use of mixture tracking capabilities. In simulation we had great experience with creating clusters of dense regions in particle space (thus for each target vehicle candidate). With having a separate cluster for each target vehicle, more robust tracking and detection can be performed. In reality however it proved hard to create and re-create meaningful clusters of particles.

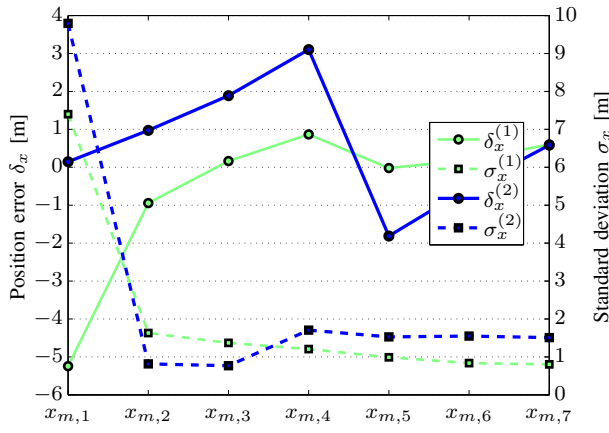
As a third extension one could think of additionally performing classification of target vehicles (like car, truck or motorbike) by the use of different dynamics and measurement models.

ACKNOWLEDGMENT

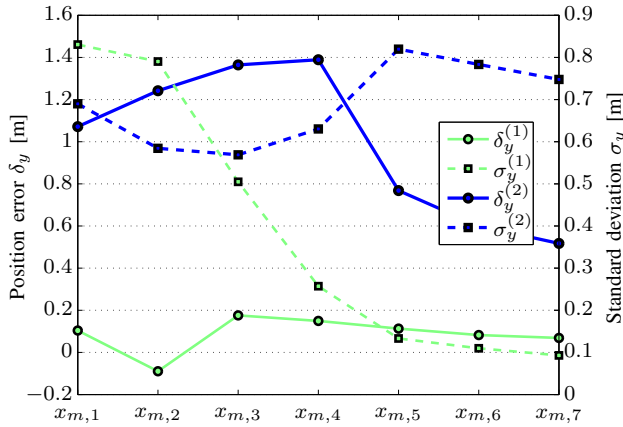
We'd like to express our gratitude to Valeo S.A. who provided the dataset used for experimental evaluation.

REFERENCES

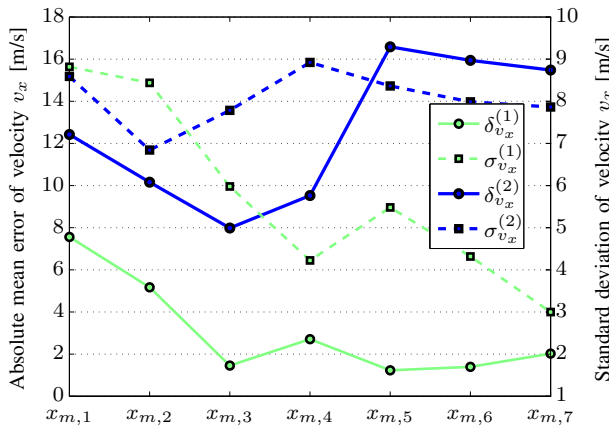
- [1] S. Thrun, "Winning the darpa grand challenge," in *Knowledge Discovery in Databases: PKDD 2006*. Springer Berlin/Heidelberg, Sept. 2006, pp. 4-4.



(a) x-position



(b) y-position



(c) velocity v_x

Fig. 8. Mean error and standard deviation of the particle filters estimate during tracking process. Reference values were taken at seven equally spaced positions $x_{m,1} \dots x_{m,7}$ with the target car entering the FOV from behind. A total number of 41 cases are included in the evaluation. Charts denoted with (1) depict results of the presented algorithm, results denoted with (2) were generated by a standard particle filter without sensor reliability model and weight-scaling.

- [2] U. Ozguner, C. Stiller, and K. Redmill, “Systems for safety and autonomous behavior in cars: The darpa grand challenge experience,” *Proc. IEEE*, vol. 95, no. 2, pp. 397–412, Feb. 2007.
- [3] M. Buehler, K. Iagnemma, and S. Singh, *The 2005 DARPA Grand Challenge: The Great Robot Race*, ser. Springer Tracts in Advanced Robotics. Springer Berlin/Heidelberg, 2007.
- [4] J. Wille and T. Form, “Realizing complex autonomous driving ma-

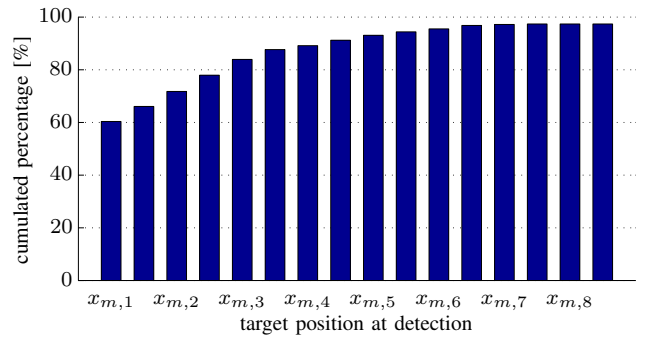


Fig. 9. Cumulated percentage of target vehicles detected in blind spot area upto denoted position. A testset of 221 km driven on motorways containing 535 BSD-cases underlies this statistics. A false alarm rate of 6.96% was achieved.

- nevers the approach taken by team carolo at the darpa urban challenge,” in *Vehicular Electronics and Safety, 2008. ICVES 2008. IEEE International Conference on*, Columbus, Ohio, USA, Sept. 2008, pp. 232–236.
- [5] C. Crane, D. Armstrong, A. Arroyo, A. Baker, D. Dankel, G. Garcia, N. Johnson, J. Lee, S. Ridgeway, E. Schwartz, E. Thorn, S. Velat, and J. H. Yoon, “Development of the navigator for the 2007 darpa urban challenge,” in *Experience from the DARPA Urban Challenge*, C. Rouff and M. Hinchey, Eds. Springer London, 2012, pp. 67–90.
- [6] J. Markoff, “Google cars drive themselves, in traffic,” *The New York Times*, vol. 10, p. A1, Oct. 2010.
- [7] F. Küçükay and J. Bergholz, “Driver assistant systems,” in *Int. Conf. on Automotive Technologies*, Istanbul, Turkey, Nov. 2004.
- [8] W. Liu, X. Wen, B. Duan, H. Yuan, and N. Wang, “Rear vehicle detection and tracking for lane change assist,” in *Intelligent Vehicles Symposium, 2007 IEEE*, Istanbul, Turkey, June 2007, pp. 252–257.
- [9] P. Batavia, D. Pomerleau, and C. Thorpe, “Overtaking vehicle detection using implicit optical flow,” in *Proceedings of the IEEE Conference on Intelligent Transportation Systems (ITSC’97)*, Boston, Massachusetts, USA, Nov 1997, pp. 729–734.
- [10] J. C. Reed, “Side zone automotive radar,” in *Proc. IEEE National Radar Conf.*, Syracuse, New York, USA, May 1997, pp. 186–190.
- [11] W.-J. Park, B.-S. Kim, D.-E. Seo, D.-S. Kim, and K.-H. Lee, “Parking space detection using ultrasonic sensor in parking assistance system,” in *Intelligent Vehicles Symposium, 2008 IEEE*, Eindhoven, Netherlands, June 2008, pp. 1039–1044.
- [12] K.-T. Song, C.-H. Chen, and C.-H. C. Huang, “Design and experimental study of an ultrasonic sensor system for lateral collision avoidance at low speeds,” in *Proc. IEEE Intelligent Vehicles Symp*, Parma, Italy, June 2004, pp. 647–652.
- [13] C. Connette, J. Fischer, B. Maidel, F. Mirus, S. Nilsson, K. Pfeiffer, A. Verl, A. Durbec, B. Ewert, T. Haar, *et al.*, “Rapid detection of fast objects in highly dynamic outdoor environments using cost-efficient sensors,” *ROBOTIK 2012*, May 2012.
- [14] F. Mirus, J. Pfadt, C. Connette, B. Ewert, D. Grüdl, and A. Verl, “Detection of moving and stationary objects at high velocities using cost-efficient sensors, curve-fitting and neural networks,” in *Proc. of the International Conference on Intelligent Robots and Systems (IROS)*, Vilamoura, Algarve, Portugal, Oct. 2012.
- [15] A. Doucet, N. Defreitas, and N. Gordon, *Sequential Monte Carlo Methods in Practice (Statistics for Engineering and Information Science)*, 1st ed. Springer New York, June 2001.
- [16] J. Vermaak, A. Doucet, and P. Perez, “Maintaining multimodality through mixture tracking,” in *Proc. Ninth IEEE Int Computer Vision Conf*, Nice, France, Oct. 2003, pp. 1110–1116.
- [17] S. Thrun, W. Burgard, and D. Fox, *Probabilistic Robotics*, ser. Intelligent Robotics and Autonomous Agents. MIT Press, 2005.
- [18] A. Petrovskaya and S. Thrun, “Model based vehicle tracking in urban environments,” in *IEEE International Conference on Robotics and Automation*, Kobe, Japan, May 2009, pp. 1–8.
- [19] L. Zhao and C. Thorpe, “Qualitative and quantitative car tracking from a range image sequence,” in *Proc. IEEE Computer Society Conf. Computer Vision and Pattern Recognition*, Santa Barbara, California, USA, June 1998, pp. 496–501.